Available at
www.ElsevierComputerScience.com
POWERED BY SCIENCE DIRECT

Signal Processing 86 (2006) 2407–2425

SIGNAL PROCESSING

www.elsevier.com/locate/sigpro

Detection of fading overlapping multipath components ☆

Nabil R. Yousef, Ali H. Sayed*, Nima Khajehnouri*,[1]

Department of Electrical Engineering, University of California Los Angeles, CA 90095-1594, USA

Received 17 June 2005; accepted 7 November 2005
Available online 13 December 2005

Abstract

Overlapping multipath propagation is one of the main sources of mobile-positioning errors, especially in fast channel fading situations. In this paper we present a technique for detecting the existence of overlapping fading multipath components. Such information is vital for accurate resolving of overlapping multipath components as well as avoiding unnecessary computations and errors in single-path propagation cases. The proposed algorithm exploits the property that fading multipath components fade independently. An analysis of the proposed technique is performed to validate its functionality and to select the algorithm parameters. The paper also presents simulation results that show a high ability of the proposed technique to detect overlapping multipath components along with its impact on the accuracy of multipath resolving techniques.

Keywords: Wireless location; Mobile positioning system; Overlapping rays; Multipath; Fading; CDMA

1. Introduction

Mobile-positioning is an essential feature of future cellular systems; it enables the positioning of cellular users in emergency 911 (E-911) situations (see, e.g., [1]). A government mandate for such services, given in [2], has led to the investigation of numerous mobile-positioning systems (e.g., [3–11]). Such systems have many other applications, besides E-911 public safety, such as location sensitive billing, fraud protection, mobile yellow pages, and fleet management (see, e.g., [12–18]).

In infrastructure-based mobile-positioning systems, the accurate estimation of the time and amplitude of arrival of the first arriving ray at the receiver(s) is vital [3,19]. Such estimates are used to obtain an estimate of the distance between the transmitter and the receiver(s). However, wireless propagation usually suffers from severe multipath conditions. In many cases, the prompt ray is succeeded by a multipath component that arrives at the receiver(s) within a short delay. If this delay is smaller than the duration of the pulse-shape used in the wireless system (the chip duration T_c in CDMA

☆This material was based on work supported in part by the National Science Foundation under awards CCR–0208573 and ECS-0401188. Part of this work appeared before in [32].
*Corresponding authors. Tel.: +1 310 267 2142; fax: +1 310 206 8495.
E-mail addresses: nyousef@newportmediainc.com (N.R. Yousef), sayed@ee.ucla.edu (A.H. Sayed), nimakh@ee.ucla.edu (N. Khajehnouri).
[1]N.R. Yousef was with the Electrical Engineering Dept. at UCLA, Los Angeles, CA. He is now with Newport Media Inc., Lake Forest, CA 92630. N. Khajehnouri and A.H. Sayed are with the Department of Electrical Engineering, University of California, Los Angeles, CA 90095, USA.

0165-1684/$ - see front matter
doi:10.1016/j.sigpro.2005.11.002

systems), then the two rays will overlap causing significant errors in the prompt ray time and amplitude of arrival estimation (see, e.g., [19]).

Fig. 1 shows the combined impulse response of a two ray channel and a conventional pulse-shape, for a CDMA IS-95 system, in two cases (a,b). In case (a), the delay between the two channel rays is equal to twice the chip duration ($2T_c$). It is clear that the peaks of both rays are resolvable, thus allowing relatively accurate estimation of the prompt ray time and amplitude of arrival. However, in case (b), both multipath components overlap and are *nonresolvable* by means of a peak-picking procedure. This can lead to significant errors in the prompt ray time and amplitude of arrival estimation.

Several works in the literature have addressed the problem of resolving overlapped multipath components by using constrained least-squares methods, which exploit the known pulse-shape (see, e.g., [20–25]). However, these methods introduce additional errors due to noise enhancement that arises from the ill-conditioning of the matrices involved in the least-squares operation, especially in fading conditions that prohibit long averaging intervals (see [25] for more details).

The main contribution of this paper is to propose and analyze a technique for detecting overlapping fading multipath components for mobile-positioning systems. The technique is based on exploiting the fact that overlapping multipath components *fade independently* (see, e.g., [26]). The method is based on defining and comparing two cost functions. The two functions coincide for single-path propagation, while a difference is detected under multipath conditions.

For simplicity of presentation, and due to space limitations, we only consider the case of *two* overlapping rays. This does not mean that the channel under consideration has only two rays; it can have many rays. However, only one ray is assumed to be close to the prompt ray by less than the pulse-shaping waveform width. In other words, we consider the case of one nonresolvable ray and many resolvable rays. Actually, the probability of having more than two channel rays within the prompt ray pulse-shaping waveform duration is relatively low. We also focus on the case of code division multiple access (CDMA) systems. We should mention that the paper provides a method for *detecting* overlapping multipath existence; its purpose is not to provide a method for TOA estimation; a problem that has been studied before in the literature (e.g., [27]).

The paper is organized as follows. In the next section, we formulate the problem addressed in the

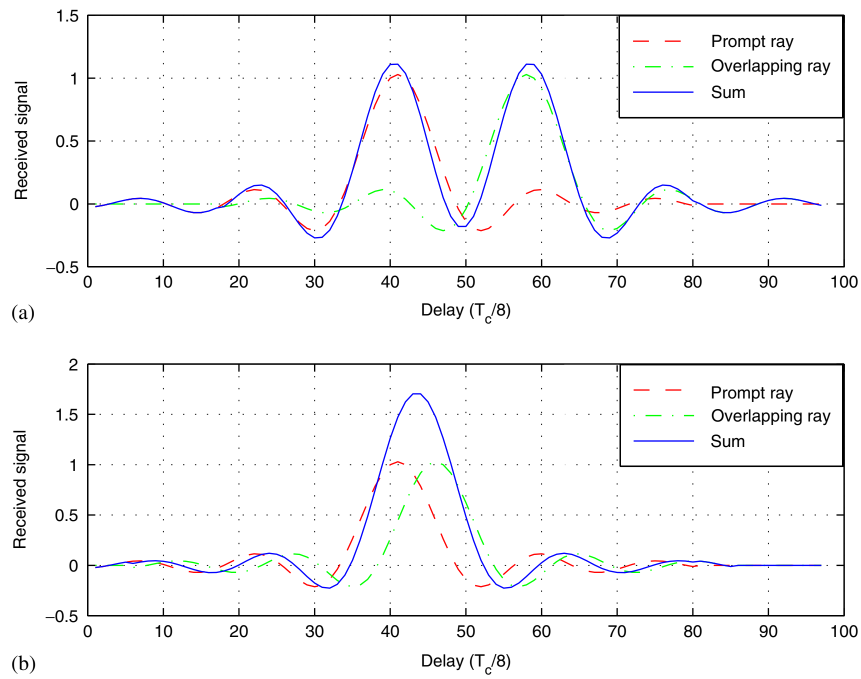

Fig. 1. Overlapping pulse-shaped rays: (a) Delay = $2T_c$. (b) Delay = $T_c/2$.

paper. In Section 3, we present the technique for detecting overlapping fading multipath components for mobile-positioning systems. The technique is justified and analyzed in Section 4 to arrive at optimal choices for the algorithm parameters, given in Section 5. In Section 6, the performance of the proposed algorithm is demonstrated by simulations in various cases; they show the ability of the proposed technique to detect overlapping multipath components. Future extensions and conclusions of the paper are given in Section 8.

2. Problem formulation

Consider a received sequence $\{r(n)\}$ that arises from a model of the form

$$r(n) = c(n) * p(n) * h(n) + v(n), \tag{1}$$

where $*$ denotes convolution, $\{c(n)\}$ is a known binary sequence, $\{p(n)\}$ is a known pulse-shape waveform sequence, $v(n)$ is zero-mean additive white Gaussian noise of variance σ_v^2, and $h(n)$ denotes the impulse response of a multipath channel with taps

$$h(n) = \sum_{l=1}^{L} \alpha_l x_l(n) \delta(n - \tau_l^o), \tag{2}$$

where $\{\alpha_l\}$ and $\{x_l(n)\}$ are, respectively, the unknown standard deviations (or gains) and the normalized amplitude coefficients; they model the Rayleigh fading nature of the channel. Several of the gains $\{\alpha_l\}$ might be zero; and a nonzero gain at some $l = l^o$ would indicate the presence of a channel ray at the corresponding delay $n = \tau_l^o$. Without loss of generality, we will assume that

$$\tau_1^o < \tau_2^o < \cdots < \tau_L^o.$$

A multipath fading channel is composed of the plurality of signal reflections, which arrive at the receiver at different delays. These different delays are affected by the relative positions of the transmitter, receiver and reflectors. In handset-based wireless location applications, the wireless base station is the transmitter, and the mobile is the receiver. In such environments, the mobile is usually surrounded by nearby reflectors. The distances between theses reflectors and the mobile (few meters) are generally smaller than the distance between the base station and the mobile (up to few kilometers). Thus, a ray transmitted from the base station to the mobile suffers several reflections from nearby reflectors. All these reflections arrive at the mobile within a very short delay of each other, with respect to the delay from the base station to the mobile (say τ_1^o). The reflections add constructively and destructively at the mobile (Rayleigh fading is an adequate model that represents this case for large enough number of reflectors).

Now, consider another ray that travels from the base station away from the mobile, hits a far away reflector (mountain or tall building), travels an extra distance till it reaches the vicinity of the mobile (say at τ_2^o). This second ray can also reflect off reflectors in the vicinity of the mobile, resulting in several reflections that arrive at the mobile around τ_2^o. In this way, we can model the channel as two (or more) fading rays at different distinct delays as in (2).

Our objective is to estimate the time-of-arrival od the *prompt* ray, τ_1^o, using the received data $\{r(n)\}$. In the case of static (i.e., non-fading) channels, a common way for estimating τ_1^o in the context of CDMA communications is as follows. Let

$$s(n) = c(n) * p(n) \tag{3}$$

denote the pulse-shaped code sequence, assumed known. We would then correlate the received sequence $r(n)$ with delayed replicas of $s(n)$ over a dense grid of possible values of τ. This correlation is done over a period of N samples of the received sequence, to obtain the following function of τ,

$$J(\tau) \triangleq \frac{1}{N} \sum_{n=1}^{N} r(n)s(n-\tau). \tag{4}$$

If the channel has only one ray, say at τ_1^o, it is known that $J(\tau)$ attains a maximum at $\tau = \tau_1^o$, which is the time of arrival of the single ray [28,29].

When, on the other hand, the channel is fading, then the correlation operation described above cannot be extended for the whole length of the received sequence, $r(n)$, as this would cause the correlation output to degrade due to the random variations of the fading channel phase. For this reason, the correlation would instead be performed over a period of N samples during which the fading channel does not vary appreciably. The phase of the correlation over these N samples would be squaring and the procedure would be repeated over the next N samples and so on. In other words, in the fading channel case, we would replace (4) by

$$J(\tau) = \frac{1}{M} \sum_{m=1}^{M} \left| \frac{1}{N} \sum_{n=n_0}^{mN} r(n)s(n-\tau) \right|^2, \tag{5}$$

where[2] $n_0 \triangleq n_0(m) = (m-1)N + 1$, and the length of the received sequence, $\{r(n)\}$, is now assumed equal to NM. This procedure is known as coherent/noncoherent averaging [27].

It was shown in [27] that the time of arrival of the first arriving ray, τ_1^o, can be obtained by estimating the index of the earliest peak of $J(\tau)$. This algorithm was shown to be successful in estimating the time of arrival of the prompt ray *only* if the difference between the prompt ray delay, τ_1^o, and the delay of the succeeding ray, τ_2^o, is larger than the chip duration T_c. If this condition is not satisfied, then picking the first peak of $J(\tau)$ could lead to significant errors in estimating, τ_1^o, as indicated in part b of Fig. 1. This is because two adjacent pulse-shaped rays would overlap with each other and the peak-picking procedure would lead to an erroneous estimate $\hat{\tau}_1^o$. Thus it is important to detect whether adjacent rays overlap with each other.

Multipath components overlapping with the prompt ray can be resolved using least-squares methods that exploit the known pulse-shape waveform (see, e.g., [20,22,25]). Such methods tend to be sensitive to data ill-conditioning. If it could be ascertained that no multipath components are detected in the vicinity of the prompt ray, then the least-squares operation could be avoided, thus eliminating errors due to ill-conditioning and saving unnecessary complexity. The contribution of this paper is to develop a technique for detecting the existence of fading multipath components overlapping with the prompt ray. If the result of the detection analysis is that no overlapping components exist, then one could proceed with the peak-picking procedure that is based on (5) in order to estimate τ_1^o. If, on the other hand, the detection analysis indicates the existence of overlapping rays, then a more sophisticated estimation procedure is needed in order to resolve/separate the rays and estimate τ_1^o accurately. A high resolution adaptive technique for performing overlapping multipath resolution and for combatting data ill-conditioning in such cases is described in [25].

3. The proposed detection technique

We first summarize the proposed method for multipath detection in wireless environments and then proceed in the next section to analyze the method and to explain the reasoning behind it. For simplicity, we focus on the case of only two overlapping rays in the vicinity of the first peak of $J(\tau)$. In the sequel, we shall use the term "*detection*" to refer to determining if the number of multipath components within the vicinity of the first peak of $J(\tau)$ is *equal to* or *more than* one. For example, if more than one ray exist, then overlapping multipath components are *detected*. The proposed method exploits the fact that different multipath rays fade independently, i.e., it exploits the following property [26]:

$$E[x_i(n)x_j^*(n)] = 1, \quad i = j, \qquad = 0, \quad i \neq j. \tag{6}$$

We first explain the intuition behind the proposed algorithm. Consider the case of a noiseless single path fading channel that consists of a single delay τ_1^o. The peak of $J(\tau)$ in (5) will occur at the location $\tau_p = \tau_1^o$. Moreover, and due to the symmetry of the pulse-shaping waveform, the function $J(\tau)$, will have the following symmetry property:

$$J(\tau_p + \delta\tau) = J(\tau_p - \delta\tau), \tag{7}$$

i.e.,

$$\begin{aligned}
&\frac{1}{M}\sum_{m=1}^{M}\left|\frac{1}{N}\sum_{n=n_0}^{mN} r(n)s(n-\tau_p-\delta\tau)\right|^2 \\
&= \frac{1}{M}\sum_{m=1}^{M}\left|\frac{1}{N}\sum_{n=n_0}^{mN} r(n)s(n-\tau_p+\delta\tau)\right|^2 \\
&= \frac{1}{M}\sum_{m=1}^{M}\left(\left[\frac{1}{N}\sum_{n=n_0}^{mN} r(n)s(n-\tau_p+\delta\tau)\right]\right. \\
&\qquad \left.\times\left[\frac{1}{N}\sum_{n=n_0}^{mN} r(n)s(n-\tau_p-\delta\tau)\right]^*\right),
\end{aligned}$$

where '*' denotes complex conjugation. In other words, due to the symmetry of $p(n)$, the cost function, $J(\tau)$, is also symmetric around τ_p. Thus, the value of $J(\tau_p + \delta\tau)$ can be obtained by any of three different operations: (i) by averaging the squared partial correlations of N samples of the received sequence, $r(n)$, with $s(n-\tau_p-\delta\tau)$, (ii) by averaging similar squared partial correlations with $s(n-\tau_p+\delta\tau)$, (iii) or by averaging the product of the partial correlations with $s(n-\tau_p-\delta\tau)$ and $s(n-\tau_p+\delta\tau)$. Let J_{product} denote the value obtained

[2]Note that throughout the paper, we will write n_0 instead of $n_0(m)$ for ease of notation.

using the third operation, i.e.,

$$J_{\text{product}} = \frac{1}{M}\sum_{m=1}^{M}\left(\left[\frac{1}{N}\sum_{n=n_0}^{mN} r(n)s(n-\tau_p+\delta\tau)\right] \times \left[\frac{1}{N}\sum_{n=n_0}^{mN} r(n)s(n-\tau_p-\delta\tau)\right]^*\right).$$

Thus, in the case of noiseless single path propagation, we have

$$J(\tau_p+\delta\tau) = J(\tau_p-\delta\tau) = J_{\text{product}}.$$

In the case of overlapping fading multipath propagation, as will be argued later in the paper, the above equalities will not hold since the three expressions, $J(\tau_p+\delta\tau)$, $J(\tau_p-\delta\tau)$, and J_{product}, will contain cross terms of *different* multipath components, as well as some other squared terms. Since different rays fade *independently*, we expect the cross terms to vanish under expectation leaving only the squared terms. Thus, we would expect a difference to exist between J_{product} and each of $J(\tau_p+\delta\tau)$ and $J(\tau_p-\delta\tau)$ in the multipath propagation case. We will base our proposed algorithm on this observation, i.e., on detecting this difference. Specifically, we will focus on the difference $J(\tau_p+\delta\tau)+J(\tau_p-\delta\tau)-2J_{\text{product}}$ and show that it will generally be positive for overlapping multipath propagation and zero otherwise.

We now describe the proposed detection algorithm in more details. The steps of the algorithm are as follows:

(1) A power delay profile (PDP), $J(\tau)$, of the received sequence, $\{r(n)\}$, is computed as defined by (5).

(2) We keep values of $J(\tau)$ within a window of twice the chip duration ($2T_{\text{c}}$) around the first peak and discard values of $J(\tau)$ outside this window range. That is, we focus mainly on detecting overlapping rays within the interval

$$\tau_p - T_{\text{c}} < \tau < \tau_p + T_{\text{c}}, \tag{8}$$

where τ_p is the index of the first peak of $J(\tau)$,

$$\tau_p = \max_{\tau} J(\tau). \tag{9}$$

This is because rays separated by more than T_{c} are resolvable by peak-picking techniques since the width of the main lobe of a CDMA pulse-shaping waveform is conventionally chosen to be equal to the chip duration (T_{c}). Note also that the number of delays inside the search window defined by (8) is equal to $2T_{\text{c}}/T_{\text{s}}+1$, where T_{s} denotes the sampling period of the received sequence $\{r(n)\}$ (and $T_{\text{s}} < T_{\text{c}}$).

(3) Two cost functions (C_{s} and C_{m}) are computed and compared. These two functions are defined such that their values are different if multiple rays exist within the vicinity of the first peak, and their values coincide for single path propagation. Thus let

$$J_{\text{s}}(\delta\tau) \triangleq J(\tau_p+\delta\tau)+J(\tau_p-\delta\tau) \tag{10}$$

and

$$J_{\text{m}}(\delta\tau) = 2J_{\text{product}} \tag{11}$$

and define

$$C_{\text{s}} \triangleq \frac{T_{\text{s}}}{T_{\text{c}}}\sum_{\delta\tau=T_{\text{s}}}^{T_{\text{c}}} J_{\text{s}}(\delta\tau) - \frac{2\widehat{\sigma_v^2}}{N}, \tag{12}$$

$$C_{\text{m}} \triangleq \frac{T_{\text{s}}}{T_{\text{c}}}\sum_{\delta\tau=T_{\text{s}}}^{T_{\text{c}}} J_{\text{m}}(\delta\tau), \tag{13}$$

where

$$\delta\tau = T_{\text{s}}, \quad 2T_{\text{s}}, \ldots, T_{\text{c}},$$

i.e., $\delta\tau = jT_{\text{s}}$ so that C_{s} and C_{m} amount essentially to the averaged values of $J_{\text{s}}(\delta_\tau)$ and $J_{\text{m}}(\delta_\tau)$ on a grid of values δ_τ. Moreover, the quantity $\widehat{\sigma_v^2}$ is an estimate of the noise variance σ_v^2, which can be estimated using many conventional techniques. For example, in the case of reverse-link CDMA channels, the noise variance σ_v^2 can be estimated *directly* from the received sequence $\{r(n)\}$ as

$$\widehat{\sigma_v^2} = \frac{1}{K_n}\sum_{i=1}^{K_n} |r(i)|^2,$$

for some value $K_n \leqslant NM$. This is because in the case the noise power is considerably higher than the signal power (e.g., −17 to −40 dB chip energy-to-noise ratio for IS-95 systems). A more accurate and unbiased estimate of the noise variance could be obtained by subtracting the signal power. However, this step is not needed in the context of CDMA due to the low SNR levels.

The justification behind the definitions of C_{s} and C_{m} as in (12)–(13) is discussed in the next section. Here, we give some explanations. As the previous equations show, C_{s} and C_{m} are

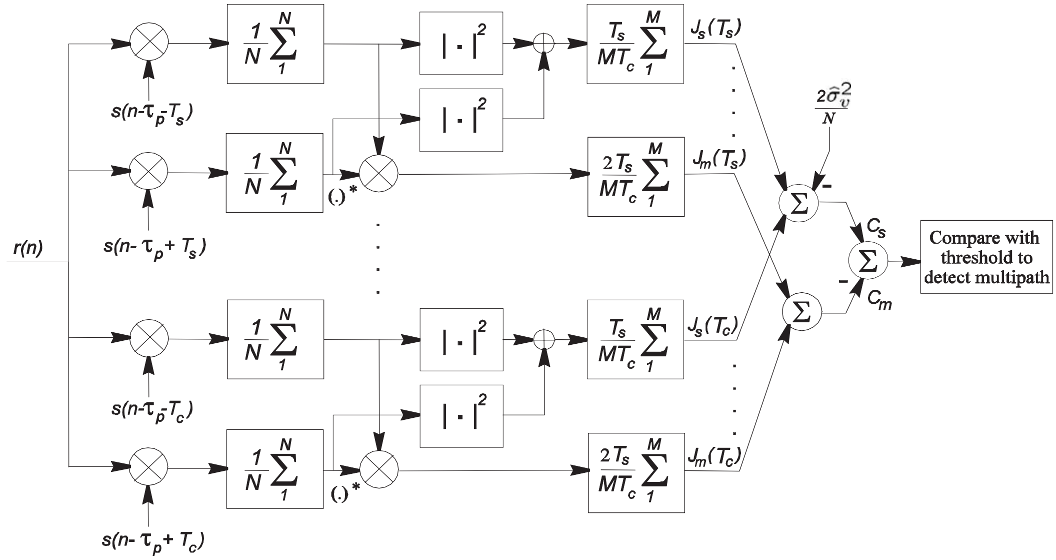

Fig. 2. Block diagram of the proposed overlapping multipath detection technique.

averaged values of the two functions $J_s(\delta\tau)$ and $J_m(\delta\tau)$, for all possible values of $\delta\tau$.[3] Thus, we would expect the difference between C_s and C_m to represent an average of the difference $J_s(\delta\tau) - J_m(\delta\tau)$ and this difference will be $J(\tau_p + \delta\tau) + J(\tau_p - \delta\tau) - 2J_{\text{product}}$ over all values $\delta\tau$, which we would expect to provide key indicator to the existence of overlapping multipath components. We will soon show that with an accurate estimate of the noise variance, C_s and C_m will be equal for single path propagation. We will also show that C_s is larger than C_m for multipath propagation. Thus, we will base our decision criterion on comparing the difference between both functions with a threshold value, β: if $C_s - C_m < \beta$, we declare that only one ray exists in the vicinity of the first peak of $J(\tau)$. However, if $C_s - C_m > \beta$, we declare that multipath propagation exists. Fig. 2 shows an implementation of the proposed algorithm.

4. Analysis and derivation

We now justify the proposed method. First, we argue that for overlapping multipath propagation, C_s is always larger than C_m, and that they coincide for single path propagation. Second, we arrive at expressions to select the algorithm parameters N and β.

We focus on the case of two overlapping multipath components, i.e., $h(n)$ has the form

$$h(n) = \alpha_1 x_1(n)\delta(n - \tau_p + \tau_1) + \alpha_2 x_2(n)\delta(n - \tau_p - \tau_2).$$

Here we are denoting, for convenience, the delays of the two rays by

$$\tau_1^o \triangleq \tau_p - \tau_1, \quad \tau_2^o \triangleq \tau_p + \tau_2, \tag{14}$$

where τ_p continues to denote the location of the first peak of $J(\tau)$. Substituting into (1) and using $s(n) = c(n) * p(n)$, the received sequence $r(n)$ can be written as

$$r(n) = \alpha_1 x_1(n) s(n - \tau_p + \tau_1) + \alpha_2 x_2(n) s(n - \tau_p - \tau_2) + v(n). \tag{15}$$

The case of single-path propagation corresponds to $\tau_1 = \tau_2 = 0$ and $x_1(n) = x_2(n)$, which leads to a single ray of delay τ_p and amplitude $\alpha = \alpha_1 + \alpha_2$.

We will consider the case of relatively long received sequence length ($M \to \infty$).[4] Then, in view of the weak law of large numbers [30], we shall assume that $J_s(\delta\tau)$ and $J_m(\delta\tau)$ in (10) and (11) can

[3] The need for subtracting the noise variance term $2\widehat{\sigma_v^2}/N$ will be explained in the next section.

[4] This is a reasonable assumption for wireless location applications, where the estimation period is in the order of a fraction of a second.

be approximated by expectations as:

$$J_{\mathrm{s}}(\delta\tau) \rightarrow_p E\left|\frac{1}{N}\sum_{n=1}^{N} r(n)s(n-\tau_p+\delta\tau)\right|^2 + E\left|\frac{1}{N}\sum_{n=1}^{N} r(n)s(n-\tau_p-\delta\tau)\right|^2$$

and

$$J_{\mathrm{m}}(\delta\tau) \rightarrow_p 2E\left(\left[\frac{1}{N}\sum_{n=n_0}^{mN} r(n)s(n-\tau_p+\delta\tau)\right] \times \left[\frac{1}{N}\sum_{n=n_0}^{mN} r(n)s(n-\tau_p-\delta\tau)\right]^*\right) \tag{16}$$

in terms of the expectation operator E and where $\rightarrow_p$ indicates convergence in probability. Using (15), we obtain

$$J_{\mathrm{s}}(\delta\tau) \rightarrow_p E\left|\frac{1}{N}\sum_{n=1}^{N}[\alpha_1 x_1(n)s(n-\tau_1^o)+\alpha_2 x_2(n) \times s(n-\tau_2^o)+v(n)]s(n-\tau_p+\delta\tau)\right|^2 + E\left|\frac{1}{N}\sum_{n=1}^{N}[\alpha_1 x_1(n)s(n-\tau_1^o) + \alpha_2 x_2(n)s(n-\tau_2^o)+v(n)]s(n-\tau_p-\delta\tau)\right|^2$$

and

$$J_{\mathrm{m}}(\delta\tau) \rightarrow_p 2E\left(\left[\frac{1}{N}\sum_{n=1}^{N}[\alpha_1 x_1(n)s(n-\tau_1^o)+\alpha_2 x_2(n) \times s(n-\tau_2^o)+v(n)]s(n-\tau_p+\delta\tau)\right] \times \left[\frac{1}{N}\sum_{n=1}^{N}[\alpha_1 x_1(n)s(n-\tau_1^o) + \alpha_2 x_2(n)s(n-\tau_2^o)+v(n)]s(n-\tau_p-\delta\tau)\right]^*\right).$$

To proceed further we make use of the following result.

Lemma 1. *Consider a sequence*

$s(n-\tau) = c(n) * p(n-\tau)$,

where $c(n)$ is a binary sequence, $p(n)$ is a pulse-shaping waveform, and τ is a delay. Given a fading channel gain sequence $\{x_j(n)\}$ whose variation within the duration of the pulse-shaping waveform is negligible, it holds that

$$\frac{1}{N}\sum_{n=1}^{N}\alpha_j x_j(n)s(n-\tau_j)s(n-\tau) \approx \alpha_j R_p(\tau-\tau_j)\frac{1}{N}\sum_{n=1}^{N}x_j(n), \tag{17}$$

where $R_p(n)$ is the autocorrelation function of the pulse-shaping waveform, defined by

$R_p(n) = p(n) * p(-n)$

and α_j is a constant gain and τ_j is a delay.

Proof. Let

$$\begin{aligned} B &\triangleq \frac{1}{N}\sum_{n=1}^{N}\alpha_j x_j(n)s(n-\tau_j)s(n-\tau) \\ &= \frac{1}{N}\sum_{n=1}^{N}\alpha_j x_j(n)[c(n)*p(n-\tau_j)]\cdot[c(n)*p(n-\tau)] \\ &= \frac{1}{N}\sum_{n=1}^{N}\alpha_j x_j(n)\left[\sum_{k=1}^{N}c(k)p(k-n+\tau_j)\right] \times \left[\sum_{q=1}^{N}c(q)p(q-n+\tau)\right] \\ &= \frac{1}{N}\sum_{n=1}^{N}\alpha_j x_j(n)\sum_{k=1}^{N}\underbrace{c(k)c(k)}_{1}p(k-n+\tau_j) \times p(k-n+\tau) \\ &\quad + \frac{1}{N}\sum_{n=1}^{N}\alpha_j x_j(n) \underbrace{\times\sum_{k=1}^{N}\sum_{q=1,q\neq k}^{N}c(k)c(q)p(k-n+\tau_j)p(q-n+\tau)}_{\approx 0}. \end{aligned} \tag{18}$$

Assuming uncorrelated weighted and shifted spreading sequences $\{c(n)\}$, the last expression in (18) can be approximated by zero and we have

$$B \approx \frac{1}{N}\sum_{n=1}^{N}\alpha_j x_j(n)\sum_{k=1}^{N}p(k-n+\tau_j)p(k-n+\tau).$$

Rewriting this term as a correlation sum, we get

$$B \approx \frac{1}{N}\alpha_j R_p(\tau-\tau_j)\sum_{n=1}^{N}x_j(n).$$

Using (17), the function $J_s(\delta\tau)$ in (17) becomes

$$J_s(\delta\tau) \to_p E\left|\frac{1}{N}\sum_{n=1}^{N}(\alpha_1 R_p(\delta\tau+\tau_1)x_1(n) + \alpha_2 R_p(\delta\tau-\tau_2)x_2(n) + v_1(n))\right|^2 + E\left|\frac{1}{N}\sum_{n=1}^{N}(\alpha_1 R_p(\delta\tau-\tau_1)x_1(n) + \alpha_2 R_p(\delta\tau+\tau_2)x_2(n) + v_2(n))\right|^2,$$

where

$$v_2(n) \triangleq v(n)\cdot s(n-\tau_p+\delta\tau),$$
$$v_1(n) \triangleq v(n)\cdot s(n-\tau_p-\delta\tau). \tag{19}$$

The noise sequence $\{v(n)\}$ in (1) is assumed to be an independent and identically (i.i.d.) process that is also independent of the channel fading gains $\{x_l(n)\}$. Note further that since the sequence $\{c(n)\}$ in the context of CDMA communications is a pseudo-noise sequence, then its samples can be assumed to be uncorrelated for all practical purposes. Moreover, $\{c(n)\}$ is also independent of the channel fading gains $\{x_l(n)\}$.

Therefore, expanding the sum (19) in $J_s(\delta\tau)$ over n, squaring, applying the expectation operator, and using (6), the expression $J_s(\delta\tau)$ reduces to

$$J_s(\delta\tau) \to_p \alpha_1^2 B_{f1}[R_p^2(\delta\tau+\tau_1) + R_p^2(\delta\tau-\tau_1)] + \alpha_2^2 \times B_{f2}[R_p^2(\delta\tau+\tau_2) + R_p^2(\delta\tau-\tau_2)] + \frac{2\sigma_{\bar{v}}^2}{N}, \tag{20}$$

where

$$B_{fj} = \frac{R_{x_j}(0)}{N} + \sum_{i=1}^{N-1}\frac{2(N-i)R_{x_j}(i)}{N^2},$$
$$R_{x_j}(i) = E[x_j(n)x_j^*(n-i)],$$
$$\sigma_{\bar{v}}^2 = \sigma_v^2 \sum_{n=1}^{N}\sum_{i=-N_p}^{N_p} p^2(n+\delta\tau+\mathrm{i}T_s)$$

and $2N_p+1$ is the number of samples in the pulse shaping filter $p(n)$. In the above, $\sigma_{\bar{v}}^2$ denotes the variance of the modified noises $\{v_1(n), v_2(n)\}$. Note that since $p(n)$ is known, then by estimating σ_v^2 we can also estimate $\sigma_{\bar{v}}^2$. However, assuming the pulse shaping filter $p(n)$ has unit energy, then $\sigma_{\bar{v}}^2$ is essentially equal to σ_v^2 and, when N is large enough, the term $\sigma_{\bar{v}}^2/N$ can be replaced by σ_v^2/N. For this reason, and for simplicity of presentation, we shall use σ_v^2 instead of $\sigma_{\bar{v}}^2$ in the sequel.

Likewise, and using similar arguments, the function $J_m(\delta\tau)$ can be expressed as

$$\begin{aligned}J_m(\delta\tau) &\to_p 2E\left(\left[\frac{1}{N}\sum_{n=1}^{N}(\alpha_1 R_p(\delta\tau-\tau_1)x_1(n) + \alpha_2 R_p(\delta\tau+\tau_2)x_2(n) + v_2(n))\right]\times\left[\frac{1}{N}\sum_{n=1}^{N}(\alpha_1 R_p(\delta\tau+\tau_1)x_1(n) + \alpha_2 R_p(\delta\tau-\tau_2)x_2(n) + v_1(n))\right]^*\right)\\ &\to_p 2E\left(\alpha_1^2 R_p(\delta\tau-\tau_1)R_p(\delta\tau+\tau_1)\left|\frac{1}{N}\sum_{n=1}^{N}x_1(n)\right|^2 + \alpha_2^2 R_p(\delta\tau-\tau_2)R_p(\delta\tau+\tau_2)\left|\frac{1}{N}\sum_{n=1}^{N}x_2(n)\right|^2\right)\\ &\to_p(\alpha_1^2 B_{f1}R_p(\delta\tau-\tau_1)R_p(\delta\tau+\tau_1) + \alpha_2^2 B_{f2}R_p(\delta\tau-\tau_2)R_p(\delta\tau+\tau_2)).\end{aligned} \tag{21}$$

The difference between the two functions, $J_s(\delta\tau)$ and $J_m(\delta\tau)$ in (20) and (21) is then given by

$$\begin{aligned}&J_s(\delta\tau) - J_m(\delta\tau)\\ &\to_p \alpha_1^2 B_{f1}[R_p^2(\delta\tau+\tau_1) + R_p^2(\delta\tau-\tau_1)] + \alpha_2^2 B_{f2}(R_p^2(\delta\tau+\tau_2) + R_p^2(\delta\tau-\tau_2)) + \frac{2\sigma_v^2}{N} - 2[\alpha_1^2 B_{f1}R_p(\delta\tau-\tau_1)R_p(\delta\tau+\tau_1) + \alpha_2^2 B_{f2}R_p(\delta\tau-\tau_2)R_p(\delta\tau+\tau_2))].\end{aligned}$$

Rearranging terms, we get

$$J_s(\delta\tau) - J_m(\delta\tau) \to_p \alpha_1^2 B_{f1}[R_p(\delta\tau+\tau_1) - R_p(\delta\tau-\tau_1)]^2 + \alpha_2^2 B_{f2}[R_p(\delta\tau+\tau_2) - R_p(\delta\tau-\tau_2)]^2 + \frac{2\sigma_v^2}{N}.$$

Thus we note that, for every $\delta\tau$,

$$\begin{aligned}&N(J_s(\delta\tau) - 2\sigma_v^2) - NJ_m(\delta\tau)\\ &\to_p \alpha_1^2 NB_{f1}[R_p(\delta\tau+\tau_1) - R_p(\delta\tau-\tau_1)]^2 + \alpha_2^2 NB_{f2}[R_p(\delta\tau+\tau_2) - R_p(\delta\tau-\tau_2)]^2 \geqslant 0\end{aligned} \tag{22}$$

and that the equality to zero occurs when $\tau_1 = \tau_2 = 0$, which corresponds to the single path propagation case. This is a useful observation since it provides a tool that can be used to distinguish between single path and multipath propagation conditions.

Now, for a finite value of M, Eq. (23) suggests that we can write

$$N(J_{\rm s}(\delta\tau) - 2\widehat{\sigma_v^2}) - NJ_{\rm m}(\delta\tau) \approx \alpha_1^2 NB_{f1}(R_p(\delta\tau+\tau_1) - R_p(\delta\tau-\tau_1))^2 + \alpha_2^2 NB_{f2}(R_p(\delta\tau+\tau_2) - R_p(\delta\tau-\tau_2))^2 + q, \quad (23)$$

where q is some random variable of variance σ_q^2, which accounts for the difference between the RHS and LHS of Eq. (23), for a finite number of samples. It also accounts for errors in $\widehat{\sigma_v^2}$. The variance of q approaches zero as $M \to \infty$.

Clearly, the value of the difference given in (23) varies with $\delta\tau$, the delay between the two rays $(\tau_1 + \tau_2)$, and the ratio between the amplitude of the two rays (α_1/α_2). Ideally, if we could determine the value of δ_τ for which the difference in (23) is a maximum, then we could compare the value of this maximum with a threshold to declare the existence or not of multipath. However, the $\{\alpha_1, \alpha_2, \alpha_3, \alpha_4\}$ are not known beforehand and, hence, we cannot determine the values of δ_{τ_o} at which the maximum occurs. A more practical and convenient approach would be the following. We evaluate the difference in (23) over a grid of values δ_τ, say over

$$T_{\rm s} \leqslant \delta_\tau \leqslant T_{\rm c} \quad (24)$$

and then average the results. This average difference is given by

$$\frac{T_{\rm s}}{T_{\rm c}} \sum_{\delta\tau=T_{\rm s}}^{T_{\rm c}} (NJ_{\rm s}(\delta\tau) - 2\hat{\sigma}_v^2 - NJ_{\rm m}(\delta\tau)) \approx \alpha_1^2 NB_{f1} \frac{T_{\rm s}}{T_{\rm c}} \sum_{\delta\tau=T_{\rm s}}^{T_{\rm c}} [R_p(\delta\tau+\tau_1) - R_p(\delta\tau-\tau_1)]^2 + \alpha_2^2 NB_{f2} \frac{T_{\rm s}}{T_{\rm c}} \sum_{\delta\tau=T_{\rm s}}^{T_{\rm c}} [R_p(\delta\tau+\tau_2) - R_p(\delta\tau-\tau_2)]^2 + q$$

again for some random variable q with variance σ_q^2. Thus, if we define

$$D \triangleq C_{\rm s} - C_{\rm m}, \quad (25)$$

with the $\{C_{\rm m}, C_{\rm s}\}$ as in (12)–(13), then

$$D = \alpha_1^2 B_{f1} \frac{T_{\rm s}}{T_{\rm c}} \sum_{\delta\tau=T_{\rm s}}^{T_{\rm c}} [R_p(\delta\tau+\tau_1) - R_p(\delta\tau-\tau_1)]^2 + \alpha_2^2 B_{f2} \frac{T_{\rm s}}{T_{\rm c}} \sum_{\delta\tau=T_{\rm s}}^{T_{\rm c}} [R_p(\delta\tau+\tau_2) - R_p(\delta\tau-\tau_2)]^2 + \frac{q}{N} \quad (26)$$

and the prior analysis shows that this difference is likely to be positive when overlapping rays exist. Comparing D with some positive threshold β would allow us to detect the presence of overlapping multipath.

5. Parameter selection

We can now select values for the parameters N and β. The value of D in (26) is composed of two terms. The first term is positive for multipath propagation and is equal to zero for single path propagation. We denote the first term by

$$C \triangleq \alpha_1^2 B_{f1} \frac{T_{\rm s}}{T_{\rm c}} \sum_{\delta\tau=T_{\rm s}}^{T_{\rm c}} [R_p(\delta\tau+\tau_1) - R_p(\delta\tau-\tau_1)]^2 + \alpha_2^2 B_{f2} \frac{T_{\rm s}}{T_{\rm c}} \sum_{\delta\tau=T_{\rm s}}^{T_{\rm c}} [R_p(\delta\tau+\tau_2) - R_p(\delta\tau-\tau_2)]^2. \quad (27)$$

The second term is a zero-mean random variable whose variance is equal to σ_q^2/N^2. Hence, $D = C +$ noise. This case resembles the problem of detecting a binary signal embedded in zero-mean additive random noise (i.e., of making a decision whether the signal is positive or zero). Of course, the accuracy of the estimation process increases with the power of the signal (C^2). The detection accuracy also decreases with the noise variance, σ_q^2/N^2. Thus, the accuracy of the detection process is improved by maximizing the *signal-to-noise* ratio, defined by

$$S \triangleq \frac{C^2}{\sigma_q^2/N^2}. \quad (28)$$

For simplicity, we will neglect the second order effect of the dependency of σ_q^2 on N. Thus, a *suboptimal* value of the parameter N is chosen as the value that maximizes S. In order to arrive at this value, we consider the case of equal maximum Doppler frequency for both rays (i.e., they have the same autocorrelation function, $R_x(i)$). In this case, the part of S that depends on N is given by $B_f^2 N^2$, where

$$B_{fj} = B_f = \frac{R_x(0)}{N} + \sum_{i=1}^{N-1} \frac{2(N-i)R_x(i)}{N^2}. \quad (29)$$

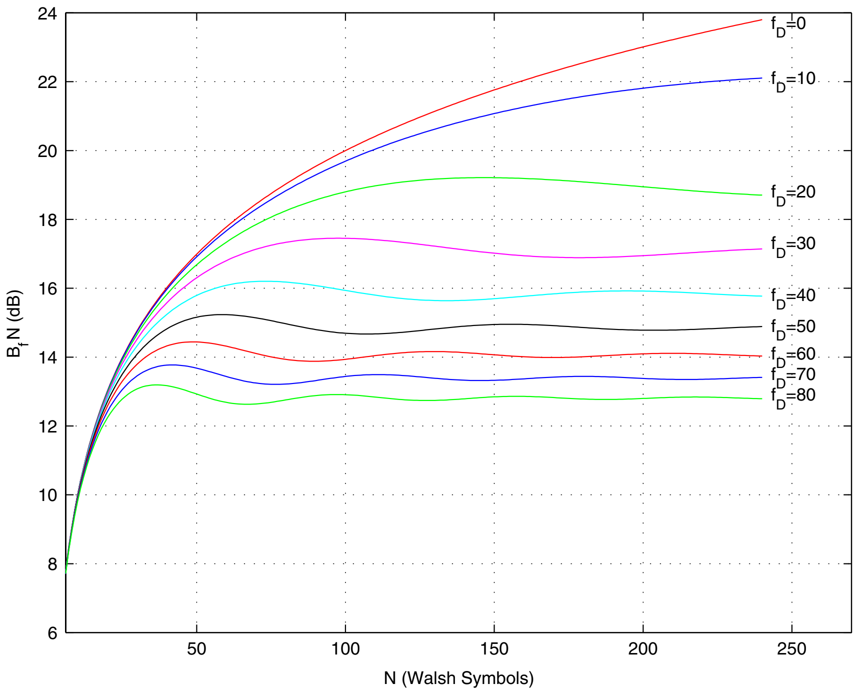

Fig. 3. $B_f N$ versus N for a Rayleigh fading channel; f_{D} is in Hz.

Fig. 3 shows a plot of $B_f N$ versus N for a Rayleigh fading channel and different values of the maximum Doppler frequency, f_{D}.[5] It can be seen that, for each f_{D}, there is a value of N, N_{opt}, that maximizes $B_f N$. Increasing N beyond this optimum value, $B_f N$ oscillates and then asymptotically approaches a fixed value that depends on f_{D}.

Since $B_f N$ is a positive function of N, then maximizing $B_f^2 N^2$ is equivalent to maximizing $B_f N$. The value of N_{opt} is computed by solving the equation

$$\frac{\mathrm{d}(B_f N)}{\mathrm{d}N} = \sum_{i=1}^{N_{\mathrm{opt}}-1} \frac{2(N_{\mathrm{opt}} - i)R_x(i) - 2N_{\mathrm{opt}} R_x(i)}{N_{\mathrm{opt}}^2} = 0 \tag{30}$$

or, equivalently,

$$\sum_{i=1}^{N_{\mathrm{opt}}-1} \mathrm{i}R_x(i) = 0. \tag{31}$$

This shows that the parameter N *should be adapted* based on the available knowledge of the channel according to (31). This is the same value of the optimal coherent integration period used in the single path searcher described in [27]. Note that for the case of Rayleigh fading channels, computing N_{opt} requires only an estimate of the channel maximum Doppler frequency, which can be obtained by using some well-known techniques (see, e.g., [31]).

We now calculate an optimal value of the threshold β. We again use the analogy with the case of estimating binary signals embedded in additive random noise. In this case, the optimal value of the threshold, β_{opt}, should be taken as half the amplitude of the signal. This choice balances the probability of detection versus the probability of false alarm. In our case, this corresponds to

$$\begin{aligned}\beta_{\mathrm{opt}} &= \frac{C}{2} \\ &= \frac{1}{2}\left(\alpha_1^2 B_{f1} \frac{T_{\mathrm{s}}}{T_{\mathrm{c}}} \sum_{\delta\tau=T_{\mathrm{s}}}^{T_{\mathrm{c}}} [R_p(\delta\tau + \tau_1) - R_p(\delta\tau - \tau_1)]^2 \right.\\ &\quad + \alpha_2^2 B_{f2} \frac{T_{\mathrm{s}}}{T_{\mathrm{c}}} \sum_{\delta\tau=T_{\mathrm{s}}}^{T_{\mathrm{c}}} [R_p(\delta\tau + \tau_2) \\ &\quad \left. - R_p(\delta\tau - \tau_2)]^2 \right).\end{aligned} \tag{32}$$

Unfortunately, since the value of the parameters τ_1, τ_2, α_1, and α_2 are not known, we are not able to

[5] In this figure, N is given in multiples of the number of samples in Walsh symbol period in a typical IS-95 system, which is 64.

calculate the value of β_{opt}. Thus, we will use a different approach to select the threshold β. First, however, let us highlight some properties of C. Fig. 4 shows C as a function of the delay between the two rays,

$$\Delta\tau \triangleq \tau_2^o - \tau_1^o = \tau_1 + \tau_2,$$

for different values of the ratio between the power of the rays, which is defined by

$$R \triangleq \frac{\alpha_1^2}{\alpha_2^2}.$$

In this figure, the maximum Doppler frequency (f_{D}) is equal to 80 Hz, N is set to the optimal value calculated from (31), and $M = 128$. The figure shows that C increases with $\Delta\tau$, for $T_{\mathrm{c}}/8 \leqslant \Delta\tau \leqslant T_{\mathrm{c}}$. This indicates the obvious conclusion that detecting sub-chip multipath components becomes easier when the delay between the two multipath components increases.

Fig. 5 shows C versus $\Delta\tau$, when $\Delta\tau$ is now extended to $2T_{\mathrm{c}}$ for $R = 0$ dB. The figure shows that detection of multipath components separated by more than a chip is also possible using our technique. However, it becomes more difficult as the delay, $\Delta\tau$, exceeds T_{c}. This range, $\Delta\tau > T_{\mathrm{c}}$, is not of much significance as rays separated by more than T_{c} are usually resolvable by peak-picking techniques.

Fig. 6 shows C versus the ratio between the power of the first and second rays (R) for three different values of $\Delta\tau$. The figure shows that C decreases with R. That is, it is easier to detect multipath components if their powers are comparable. If most of the received signal power is concentrated in one ray, it becomes more difficult to detect the existence of the other ray and vice versa. Here, we note that the knee $\Delta\tau = 5T_{\mathrm{c}}/8$ occurs due to the coarse quantization of τ_1 and τ_2 in $\Delta\tau = \tau_1 + \tau_2 = 5T_{\mathrm{c}}/8$ in units of $T_{\mathrm{c}}/8$. When R changes from 5 to 6 dB, the values of τ_1 and τ_2 change from $2T_{\mathrm{c}}/8$ and $3T_{\mathrm{c}}/8$ to $T_{\mathrm{c}}/8$ and $4T_{\mathrm{c}}/8$ causing the sudden change in the value of C.

Fig. 7 shows C versus $\Delta\tau$ for two different values of f_{D} (10 and 80 Hz) and two values of R (0 and 5 dB). The figure shows that C decreases slightly with f_{D}. However, the change in C is minor despite the wide change in f_{D}. This indicates that C is not affected greatly by the value of f_{D}. This is due to the fact that B_f does not vary much with f_{D} if N is chosen at its optimal value given in (31).

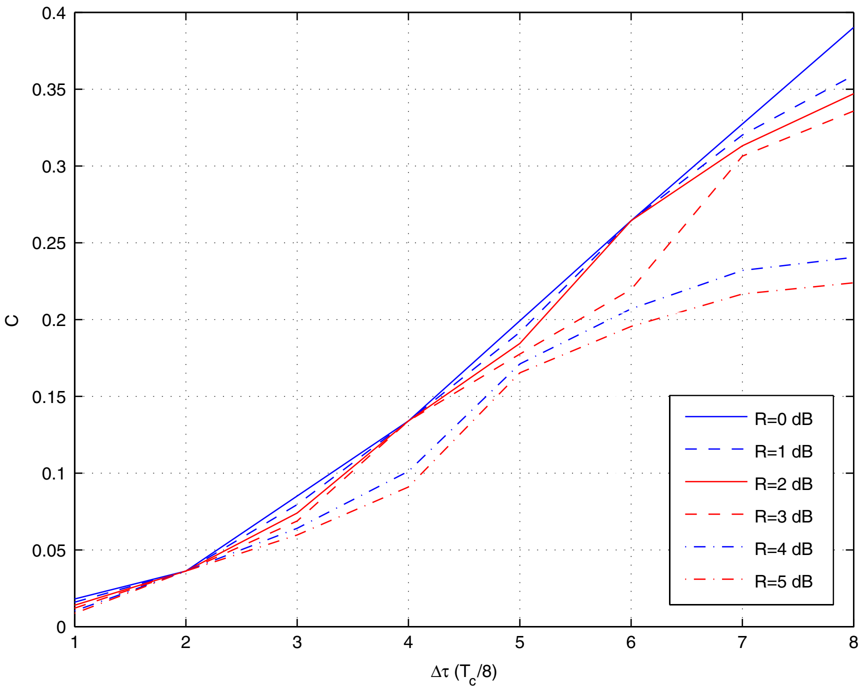

Fig. 4. C versus $\Delta\tau$ for different values of R.

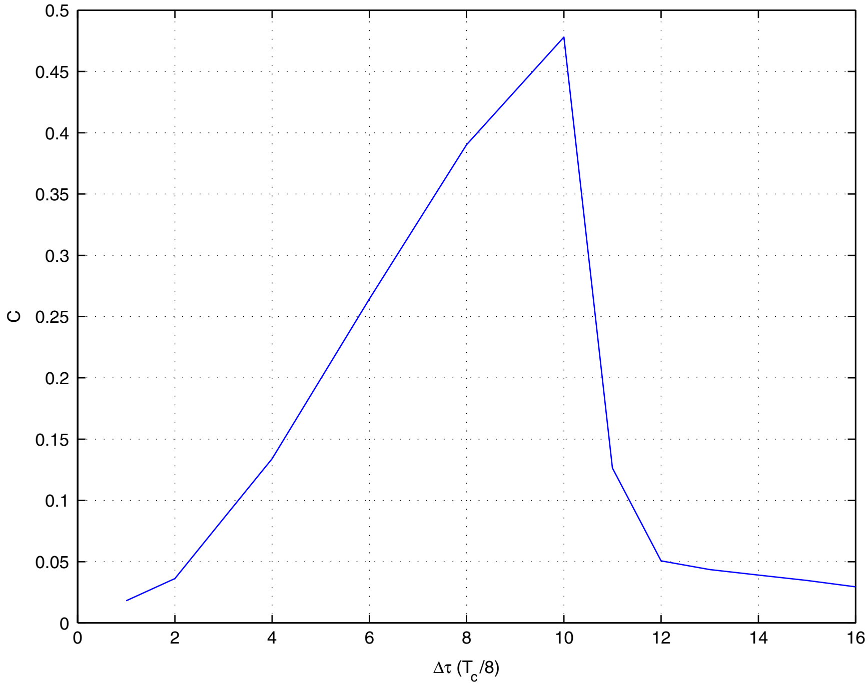

Fig. 5. C versus $\Delta\tau$.

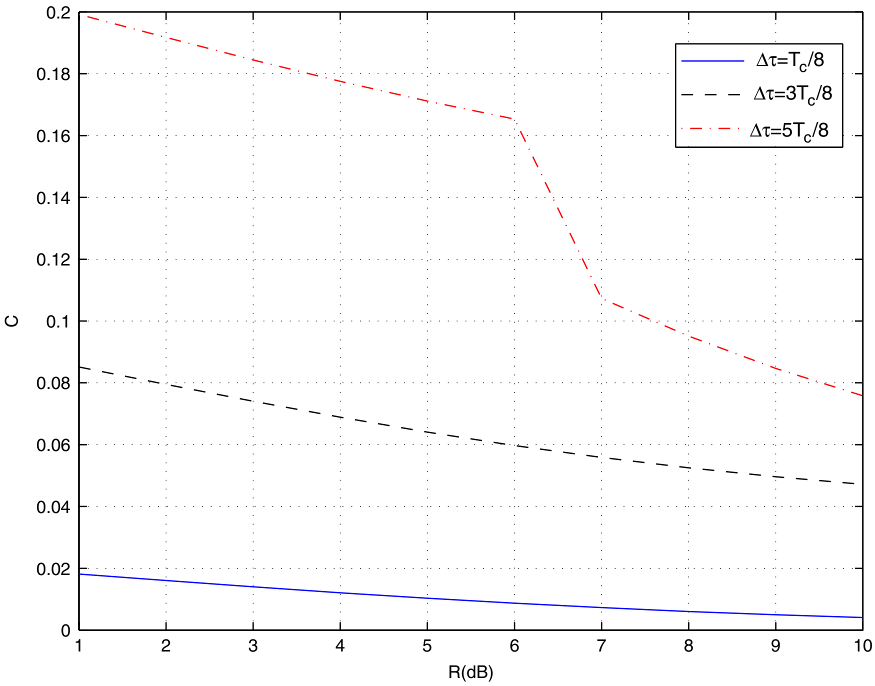

Fig. 6. C versus R for different values of $\Delta\tau$.

After investigating the properties of C, we arrive at the following observation. The value of C and the optimal threshold, β_{opt}, both decrease with decreasing the delay between the two multipath components, $\Delta\tau$, and with increasing the ratio between the power of the stronger ray and the power of the weaker ray. In fact, C goes to zero if $\Delta\tau \to 0$ or $R \to \infty$. This is expected as both cases correspond

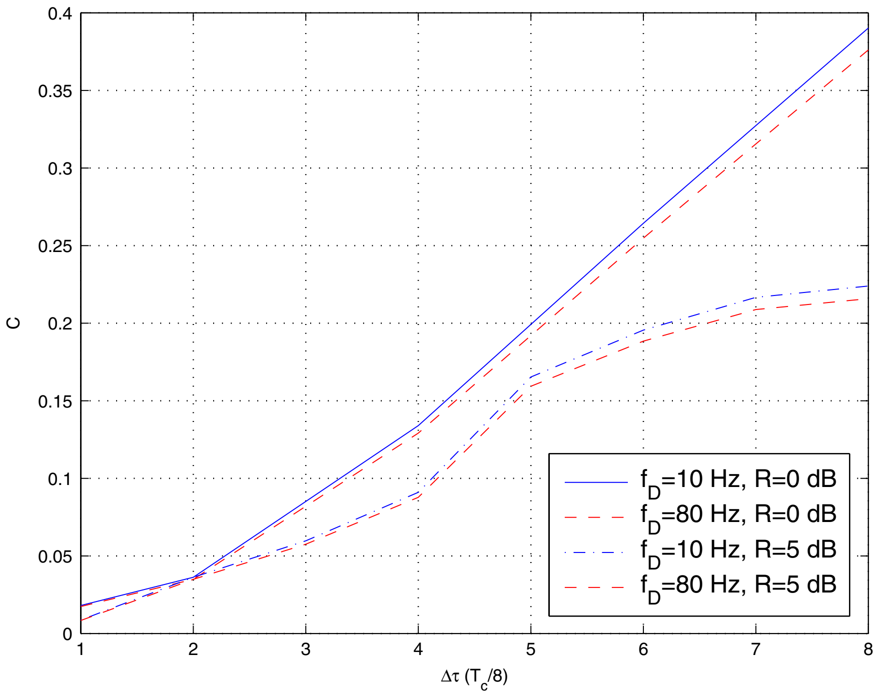

Fig. 7. C versus $\Delta\tau$ for different values of f_{D} and R.

to the case of single path propagation. Thus, in order to set a value for the threshold, β, we have to set a minimum delay resolution, $\Delta\tau_{\min}$, below which we do not wish to detect overlapping rays (say $T_c/8$). Rays separated by less than this delay will not be detected. Moreover, we also set a limit for the ratio between the power of the two rays ($R_{\max}$) (say 5 dB). In other words, if the power of the weaker ray is smaller than the power of the stronger ray by more than 5 dB, it will not be detected. Both $\Delta\tau_{\min}$ and $R_{\max}$ are design parameters that are based on the specific application. By setting the threshold β to this *worst case*, it becomes *robust* to the cases in which $\Delta\tau > \Delta\tau_{\min}$ and $R < R_{\max}$, i.e., we expect the probability of multipath detection to be larger in these cases.

Once we set $\Delta\tau = \Delta\tau_{\min}$ and $R = R_{\max}$, we can solve for τ_1 and τ_2 in this worst case (denoted by $\bar{\tau}_1$ and $\bar{\tau}_2$) as follows. First, we note that τ_p is given by

$$\tau_p = \arg\max_{\tau}[\alpha_1\, p(\tau - \tau_1^o) + \alpha_2\, p(\tau - \tau_2^o)].$$

Substituting $\tau_1^o = \tau_p - \tau_1$, $\tau_2^o = \tau_p + \tau_2$, $\Delta\tau = \tau_1 + \tau_2$ and $\alpha_1/\alpha_2 = \sqrt{R}$, we get

$$\begin{aligned}\tau_1^o + \tau_1 = {} & \arg\max_{\tau}(\alpha_1 p(\tau - \tau_1^o) \\ & + \alpha_1/\sqrt{R}p(\tau - \tau_1^o - \Delta\tau)).\end{aligned}$$

Since α_1 is independent of τ, we can write

$$\begin{aligned}\tau_1^o + \tau_1 = {} & \arg\max_{\tau}(p(\tau - \tau_1^o) \\ & + 1/\sqrt{R}p(\tau - \tau_1^o - \Delta\tau)).\end{aligned}$$

Without loss of generality, we can set $\tau_1^o = 0$, which leads to

$$\tau_1 = \arg\max_{\tau}(p(\tau) + 1/\sqrt{R}p(\tau - \Delta\tau)).$$

Now by setting $\Delta\tau = \Delta\tau_{\min}$ and $R = R_{\max}$, we obtain

$$\begin{aligned}\bar{\tau}_1 &= \arg\max_{\tau}\left(p(\tau) + \frac{1}{\sqrt{R_{\max}}}p(\tau - \Delta\tau_{\min})\right), \\ \bar{\tau}_2 &= \Delta\tau_{\min} + \bar{\tau}_1, \end{aligned} \tag{33}$$

where $p(\tau)$ is the pulse-shaping waveform. The ray amplitudes in this worst case design ($\bar{\alpha}_1$ and $\bar{\alpha}_2$) are then obtained from the value of the maximum of the cost function $J(\tau)$ in (5). Using (10), at $\delta\tau = 0$, we get $J_s(0) = 2J(\tau_p)$. Setting $\delta\tau = 0$ and substituting τ_1 and τ_2 by $\bar{\tau}_1$ and $\bar{\tau}_2$ in (20), we obtain

$$J(\tau_p) \to_p \bar{\alpha}_1^2 B_f R_p^2(\bar{\tau}_1) + \frac{1}{R_{\max}}\bar{\alpha}_1^2 B_f R_p^2(\bar{\tau}_2) + \frac{\sigma_v^2}{N}.$$

Thus $\bar{\alpha}_1$ and $\bar{\alpha}_2$ are approximately given by

$$\bar{\alpha}_1 \approx \sqrt{\frac{J(\tau_p) - \widehat{\sigma_v^2}/N}{B_f R_p^2(\bar{\tau}_1) + \frac{1}{R_{\max}} B_f R_p^2(\bar{\tau}_2)}},$$

$$\bar{\alpha}_2 \approx \frac{1}{\sqrt{R_{\max}}}\, \bar{\alpha}_1. \quad (34)$$

A worst case value for the threshold, β, can now be obtained by substituting (33) and (34) into (32). This value, which we denote by β_w, is given by

$$\beta_w \approx \frac{1}{2}\left(\bar{\alpha}_1^2 B_{f1} \frac{T_s}{T_c} \sum_{\delta\tau=T_s}^{T_c} (R_p(\delta\tau + \bar{\tau}_1) \quad (35)\right.$$

$$- R_p(\delta\tau - \bar{\tau}_1))^2 + \bar{\alpha}_2^2 B_{f2} \frac{T_s}{T_c}$$

$$\left. \times \sum_{\delta\tau=T_s}^{T_c} (R_p(\delta\tau + \bar{\tau}_2) - R_p(\delta\tau - \bar{\tau}_2))^2\right). \quad (36)$$

Algorithm: Given a received sequence $\{r(n)\}$ that arises from the model (15), then overlapping multipath propagation could be detected by comparing the difference D defined by

$$D \triangleq C_s - C_m,$$

where C_s and C_m are as in (12) and (13), to the threshold β_w given by (36), where T_s is the sampling period, T_c is the chipping sequence period, $\bar{\tau}_1$, $\bar{\tau}_2$, $\bar{\alpha}_1$, $\bar{\alpha}_2$, B_{f1}, and B_{f2} are given by (33), (34), and (29). The function $R_p(n)$ is the autocorrelation function of the pulse-shaping waveform, defined by

$$R_p(n) = p(n) * p(-n).$$

Moreover, the optimal value of the parameter N (denoted by N_{opt}) used in evaluating C_s and C_m that maximizes the signal-to-noise ratio is the solution of

$$\sum_{i=1}^{N_{\text{opt}}-1} iR_x(i) = 0, \quad (37)$$

where $R_x(i)$ is the autocorrelation function of the fading channel given in (15).

6. Simulation results

The performance of the proposed technique is evaluated by computer simulations. In the simulations, a typical IS-95 signal is generated, pulse-shaped, and transmitted through a multipath Rayleigh fading channel using Jakes model [26]. The total power gain of the channel components is normalized to unity, i.e., $\sum_{l=1}^{L} |\alpha_l|^2 = 1$. The delay between the two multipath components is chosen to be multiples of $T_c/8$. Both multipath components fade independently at a maximum Doppler frequency of f_D. Additive white Gaussian noise is added at the output of the channel to account for both multiple access interference and thermal noise. The received chip energy-to-noise ratio (E_c/N_o) of the input sequence, $r(n)$, is varied in the range of -10 to -20 dB, which is common for CDMA IS-95 systems.

Fig. 8 shows the single and multipath cost functions, $J_s(\delta\tau)$ and $J_m(\delta\tau)$, versus the delay index $\delta\tau$ in two cases, (a) and (b), for $E_c/N_o = -15$ dB and $f_D = 80$ Hz. In case (a), where two equal multipath components separated by $T_c/8$ exist, we can see that $J_s(\delta\tau) > J_m(\delta\tau)$. In case (b), where only one ray exists, the two cost functions coincide.

6.1. Effect of R on P_d

Fig. 9 shows the probability of multipath detection (P_d) versus E_c/N_o for four different values of the ratio between the prompt ray power and the overlapping ray power ($R(\text{d}B) = 20\log_{10}(\alpha_1/\alpha_2)$). In these simulations, the delay between the two rays is equal to $T_c/8, \beta = 0.001$, and the probability P_d is calculated as the average of 100 runs. For $R = 0$ dB (equal rays), P_d is approximately equal to unity for the chosen range of E_c/N_o. On the other hand, P_d is approximately equal to zero for $R = \infty$ (single-path propagation). Thus the proposed technique can successfully distinguish between single-path and multipath propagation, even for low values of E_c/N_o.

6.2. Effect of $\Delta\tau$ on P_d

Fig. 10 shows the probability of multipath detection (P_d) versus E_c/N_o for four different values of the delay between the two rays, $\Delta\tau$. In this simulation, the ratio between the prompt ray power and the overlapping ray power, R, is set to -5 dB for the multipath case and ∞ for the single-path case, $\beta = 0.0042$, and the probability P_d is calculated as the average of 100 runs. We can see from these results that the proposed algorithm has perfect detection probability except at very low values of E_c/N_o and $\Delta\tau$ at the edge of our design, $\Delta\tau = T_c/8$.

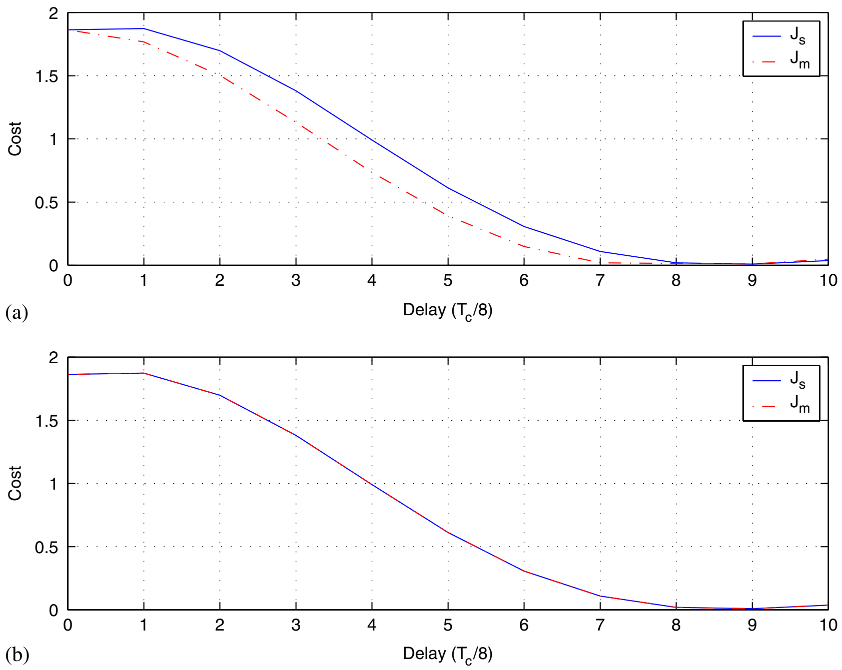

Fig. 8. Cost functions versus delay: (a) Two rays. (b) One ray.

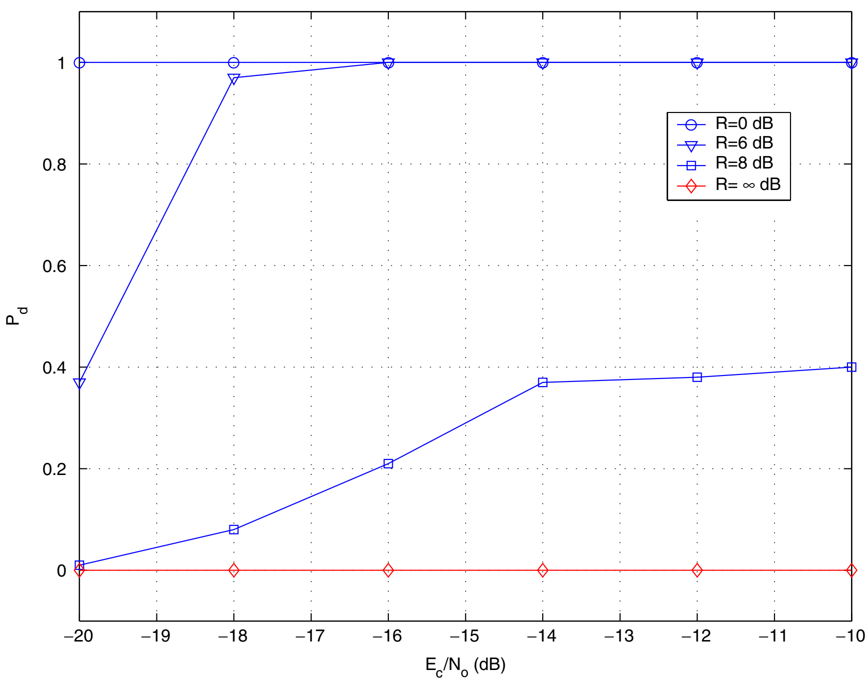

Fig. 9. Probability of multipath detection versus E_c/N_o.

6.3. Effect of M on P_d

In our analysis, we made the assumption that the length of the noncoherent integration period, M, goes to infinity, i.e., an infinitely long received sequence. It is thus desirable to check the performance of the proposed detection technique for finite length received sequences, i.e., for practical values

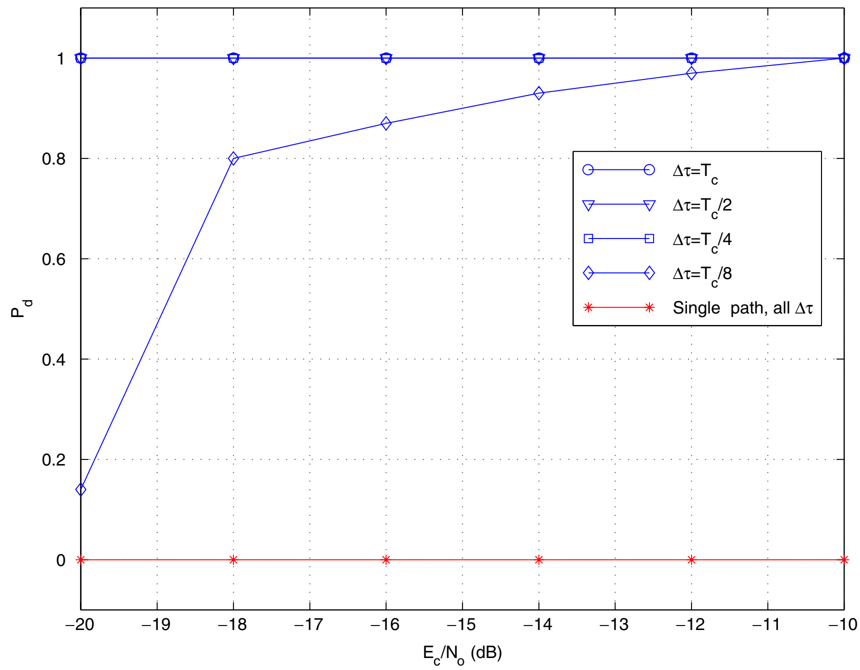

Fig. 10. Probability of multipath detection versus E_c/N_o for different values of $\Delta\tau$.

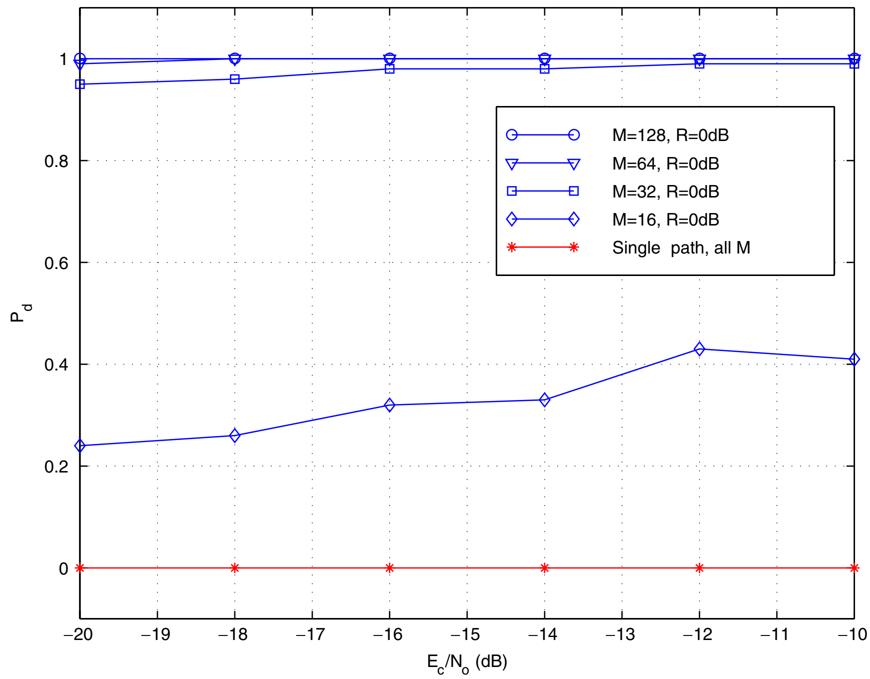

Fig. 11. Probability of multipath detection versus E_c/N_o for different values of M.

of M. Fig. 11 shows the effect of varying M on the probability of multipath detection, P_d, for multipath ($R = 0\,\mathrm{dB}$) and single-path ($R = \infty\,\mathrm{dB}$) cases, respectively. Here we can see that the precision of the detection process increases with M. This is expected as the precision of the noise variance estimate increases with M and also the assumption that the channel multipath components fade independently, which is heavily exploited in our analysis and which is given by (6), is not feasible unless a long enough received sequence is used, i.e., for long enough M. Note also that the results reflect that for the conditions described above, a very high probability of detection can be achieved for M larger than 64, which is a reasonable value in practice, i.e., it corresponds to a reasonable data collection duration (around 0.4 s in this case). Notice that for $R = \infty\,\text{dB}$, the probability of detection is zero for all considered values of M, i.e., no false alarm was ever noticed in these simulations. This is because no independent fading needs to be exploited in the single-path case, as only one ray exists. Thus, a relatively smaller value of M can guarantee that no false alarm occurs. This is in fact a useful property of the proposed detection method as a false alarm could be more damaging to the estimation process than not detecting existing overlapping multipath components.

7. Mobile-positioning application

The impact of using the a priori multipath information, obtained from the proposed algorithm, on overlapped multipath resolving techniques is reflected by the simulation results given in Fig. 12. In these results, a Rayleigh fading channel is considered. The channel has two overlapping Rayleigh fading rays with a maximum Doppler frequency of 10 Hz. The two overlapping rays are shown in the first plot of the figure. An IS-95 pulse-shaped CDMA signal is transmitted over this channel. The signal-to-noise ratio at the output of the channel is $-10\,\text{dB}$. The delay between the two rays corresponds to $T_c/4$. The second plot of Fig. 12 shows the output of a conventional matched filtering stage followed by a conventional least-squares deconvolution stage. It is clear that the amplitude of the signal at the output of such a procedure is significantly degraded leading to significant errors in the estimation of the time and amplitude of arrival of the first arriving ray. The third plot of the figure shows the estimated channel if a regularized least-squares operation is used instead of the conventional least-squares operation. Again we can see that this method fails in resolving an accurate estimate for the channel. Finally, the fourth plot of Fig. 12 shows the estimated channel when a model-based adaptive solution is used [27]. In this case, we can see that the a priori information provided by the proposed method serves to enhance the channel estimate significantly. Furthermore, we can see that conventional least-squares techniques suffer from high levels of noise enhancement. Thus, the proposed algorithm can avoid these errors in the case of single path propagation, when no overlapping multipath components are detected. Moreover, Ref. [12] overviews different methods of cellular position estimation using time-of-arrival and time-difference-of-arrival.

8. Conclusions

In this paper, we presented a technique for detecting overlapping multipath components. The proposed technique was analyzed to optimize its parameters and simulation results showed a high level of detection accuracy. Having such a priori information about the *existence* of overlapping multipath components can be useful in overcoming some challenges facing overlapping multipath resolving:

(1) If no overlapping multipath components are detected within a pulse-shape period from the prompt ray, a peak-picking operation is sufficient and no least-squares operation is needed. This avoids noise enhancement and saves unnecessary calculations. In these cases, the single path searcher of [27], for example, achieves a high accuracy for the time and amplitude of arrival estimates of the first arriving ray.
(2) If overlapping multipath components are detected, an adaptive searcher, which avoids the matrix ill-conditioning problem associated with the least-squares design, can be developed [25].
(3) Having information about the existence of overlapping multipath components could serve to provide a measure of the *degree of confidence* in the location estimation in general. Providing such level of confidence in the location process is recommended by the Federal Communications Commission (FCC) (2). For example, if no overlapping multipath components were detected in the vicinity of the first arriving ray of the MS signal at a specific BS, the level of accuracy in the estimation of the time and amplitude of arrival of the first arriving ray in this case is a function of the received signal SNR at this specific BS. It is shown in [27] that such accuracy level is high in the case of single path propagation. On the other

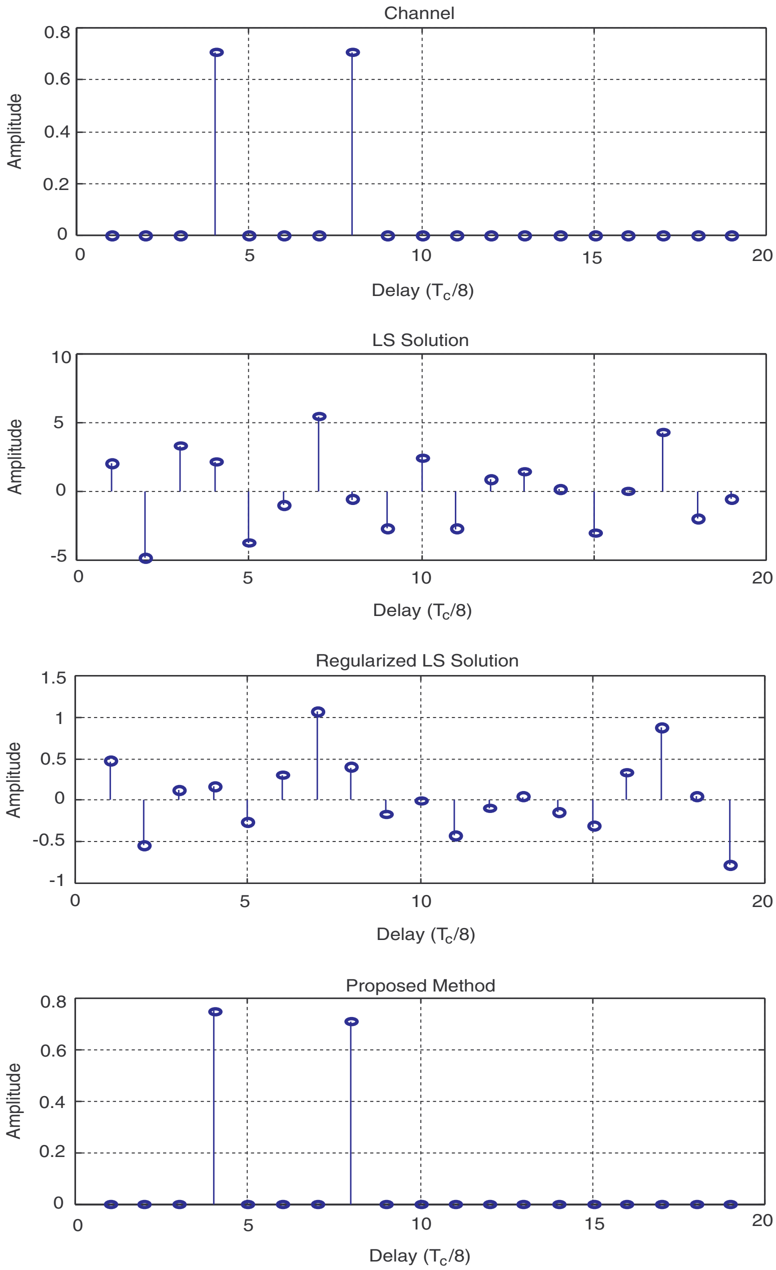

Fig. 12. Impact of using a priori multipath information on multipath resolving.

hand, if overlapping multipath components are detected, the level of accuracy in this case is dependent on the received signal SNR as well as on the ability to resolve the overlapping multipath components. In general, we expect a higher accuracy in the case of no detected overlapping multipath components.

Acknowledgements

The authors would like to thank Dr. Louay Jalloul for useful discussions on the topic of the paper, especially for bringing to their attention the potential of using correlations between different RAKE fingers.

References

[1] A.H. Sayed, A. Tarighat, N. Khajehnouri, Network-based wireless location, IEEE Signal Process. Mag. 22 (4) (July 2005) 24–40.

[2] FCC Docket No. 94-102, Revision of the commissions rules to insure compatibility with enhanced 911 emergency calling systems, Technical Report RM-8143, July 1996.

[3] J.J. Caffery, G.L. Stuber, Overview of radiolocation in CDMA cellular systems, IEEE Commun. Mag. 36 (4) (April 1998) 38–45.

[4] J. O'Connor, B. Alexander, E. Schorman, CDMA infrastructure-based location for E911, in: Proceedings of the IEEE Vehicular Technology Conference, vol. 3, Houston, TX, May 1999, pp. 1973–1978.

[5] S. Fischer, H. Koorapaty, E. Larsson, A. Kangas, System performance evaluation of mobile positioning methods, in: Proceedings of the IEEE Vehicular Technology Conference, vol. 3, Houston, TX, May 1999, pp. 1962–1966.

[6] S. Tekinay, E. Chao, R. Richton, Performance benchmarking for wireless location systems, IEEE Commun. Mag. 36 (4) (April 1998) 72–76.

[7] J. Caffery, G. Stuber, Radio location in urban CDMA microcells, in: Proceedings of the IEEE International Symposium on Personal, Indoor and Mobile Radio Communications, vol. 2, Toronto, Canada, September 1995, pp. 858–862.

[8] A. Ghosh, R. Love, Mobile station location in a DS-CDMA system, in: Proceedings of the IEEE Vehicular Technology Conference, vol. 1, May 1998, pp. 254–258.

[9] C. Drane, M. Macnaughtan, C. Scott, Positioning GSM telephones, IEEE Commun. Mag. 36 (4) (April 1998) 46–54.

[10] N.J. Thomas, D.G.M. Gruickshank, A passive mobile location system for UMTS, in: Proceedings of the IEE Colloquium on UMTS Terminals and Software Radio, Glasgow, UK, April 1999, pp. 254–258.

[11] K. Kuboi, S. Shirota, S. Sakagami, S. Aoyama, A. Akeyama, Vehicle position estimates by multibeam antennas in multipath environments, IEEE Trans. Veh. Technol. 41 (1) (February 1992) 63–68.

[12] A.H. Sayed, N.R. Yousef, Wireless location, in: J. Proakis (Ed.), Wiley Encyclopedia of Telecommunications, Wiley, NY, 2003.

[13] J.M. Zagami, S.A. Parl, J.J. Bussgang, K.D. Melillo, Providing universal location services using a wireless E911 location network, IEEE Commun. Mag. 36 (4) (April 1998) 66–71.

[14] T.S. Rappaport, J.H. Reed, B.D. Woerner, Position location using wireless communications on highways of the future, IEEE Commun. Mag. 34 (10) (October 1996) 33–41.

[15] L.A. Stilp, Carrier and end-user application for wireless location systems, in: Proceedings of SPIE, vol. 2602, Philadelphia, PA, October 1996, pp. 119–126.

[16] I. Paton, et al., Terminal self-location in mobile radio systems, in: Proceedings of the 6th International Conference on Mobile Radio and Personal Communications, Coventry, UK, vol. 1, December 1991, pp. 203–207.

[17] A. Giordano, M. Chan, H. Habal, A novel location-based service and architecture, in: Proceedings of the IEEE PIMRC, vol. 2, Toronto, Canada, September 1995, pp. 853–857.

[18] J. Caffery, G. Stuber, Vehicle location and tracking for IVHS in CDMA microcells, in: Proceedings of the IEEE International Symposium on Personal, Indoor and Mobile Radio Communications, Amsterdam, Netherlands, September 1994, vol. 4, pp. 1227–1231.

[19] J.H. Reed, K.J. Krizman, B.D. Woerner, T.S. Rappaport, An overview of the challenges and progress in meeting the E-911 requirement for location service, IEEE Commun. Mag. 36 (4) (April 1998) 30–37.

[20] Z. Kostic, M.I. Sezan, E.L. Titlebaum, Estimation of the parameters of a multipath channel using set-theoretic deconvolution, IEEE Trans. Commun. 40 (6) (June 1992) 1006–1011.

[21] Z. Kostic, G. Pavlovic, Resolving subchip-spaced multipath components in CDMA communication systems, IEEE Trans. Veh. Technol. 48 (6) (November 1999) 1803–1808.

[22] T.G. Manickam, R.J. Vaccaro, A non-iterative deconvolution method for estimating multipath channel responses, in: Proceedings of the ICASSP, vol. 1, April 1993, pp. 333–336.

[23] E. Fishler, B. Bobrovsky, Anti multipath cellular radio location for DS/CDMA systems using a novel EKF subchip RAKE tracking loop, in: IEEE Military Communications Conference Proceedings, vol. 2, 1999, pp. 1328–1332.

[24] A.W. Habboosh, R.J. Vaccaro, S. Kay, An algorithm for detecting closely spaced delay/Doppler components, in: Proceedings of the ICASSP, vol. 1, April 1997, pp. 535–538.

[25] N.R. Yousef, A.H. Sayed, N. Khajehnouri, Adaptive subchip multipath resolving for wireless location systems, EURASIP Journal on Applied Signal Processing, 2006 to appear.

[26] T. Rappaport, Wireless Communications; Principles and Practice, Prentice-Hall, Englewood Cliffs, NJ, 1996.

[27] N.R. Yousef, A.H. Sayed, L.M.A. Jalloul, Robust wireless location over fading channels, IEEE Trans. Veh. Technol. 52 (1) (January 2003) 117–126.

[28] S. Glisic, B. Vucetic, Spread Spectrum CDMA Systems for Wireless Communications, Artech House, Boston, 1997.

[29] S. Rappaport, D. Grieco, Spread-spectrum signal acquisition: Methods and technology, IEEE Commun. Mag. 22 (6) (June 1984) 6–21.

[30] R. Durrett, Probability: Theory and Examples, second ed., Duxbury Press, 1995.

[31] A. Swindlehurst, A. Jakobsson, P. Stoica, Subspace-based estimation of time delays and Doppler shifts, IEEE Trans. Signal Process. 46 (9) (September 1998) 2472–2483.

[32] N.R. Yousef, A.H. Sayed, Detection of fading overlapping multipath components for mobile-positioning systems, in: Proceedings of ICC, vol. 10, Helsinki, Finland, June 2001, pp. 3102–3106.